GSA Data Repository item 2014315

Data repository item for Kemp and Sexton (2014): Time-scale uncertainty of abrupt events in the geologic record arising from unsteady sedimentation

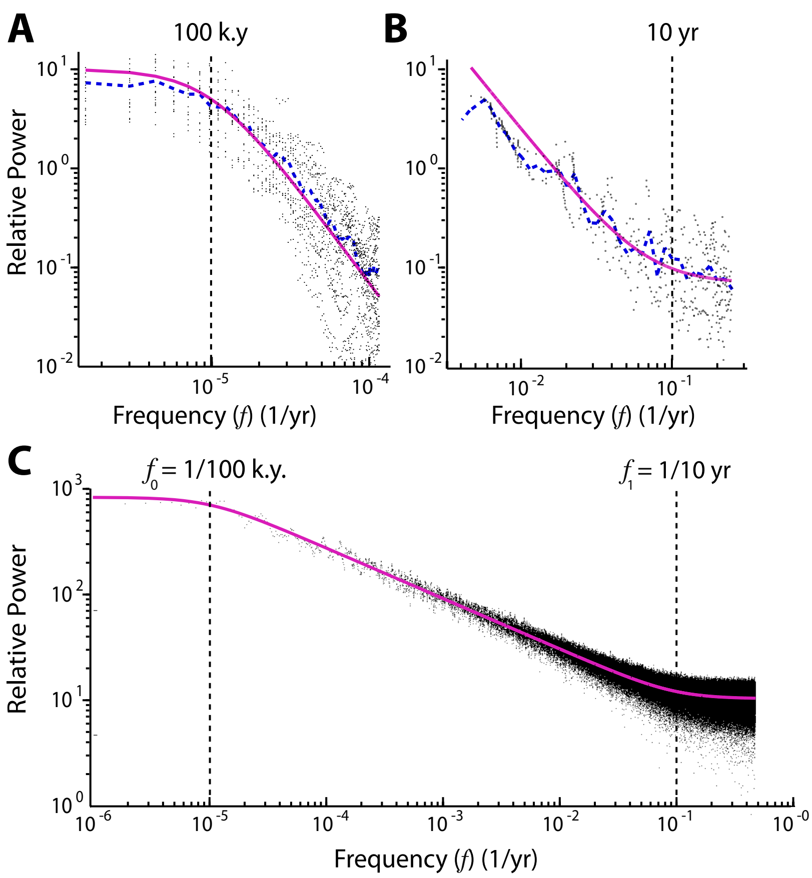

Figure DR1. A, Power spectrum of sedimentation rates from oceanic cores analysed in Huybers and Wunsch (2004). Blue dashed line is the mean of the spectral estimates. Purple line is the fit to these estimates using equation 2 of main text, with f_0 = 1/100 k.y. Redrawn from Huybers and Wunsch (2004). B, Power spectrum of varve thickness records from laminated marine sediments of the Eocene Green River Formation (data from Crowley et al., 1986). Blue dashed line is the mean of the spectral estimates. Purple line is the fit to these estimates using equation 2 of main text, with f_1 = 1/10 yr. C, Power spectrum of synthetic sedimentation rate record (1 m.y. long, sampling interval = 1 yr). This record was constructed from equations 2 and 3 of main text. Purple line is fit to this record using equation 2, with f_0 = 1/100 k.y. and f_1 = 1/10 yr. A lack of age control precludes the ability to constrain sedimentation rate variance in real successions at periods >~100 yr and <~10 k.y., and the model conservatively assumes a smooth continuous scaling of the spectrum between these periods. Note in particular the match between the slope in the spectrum of A at frequencies higher than ~10^{-5} and the slope in the spectrum of B at frequencies lower than ~10^{-1}, which supports a common scaling of variance between these frequencies, as shown in C.

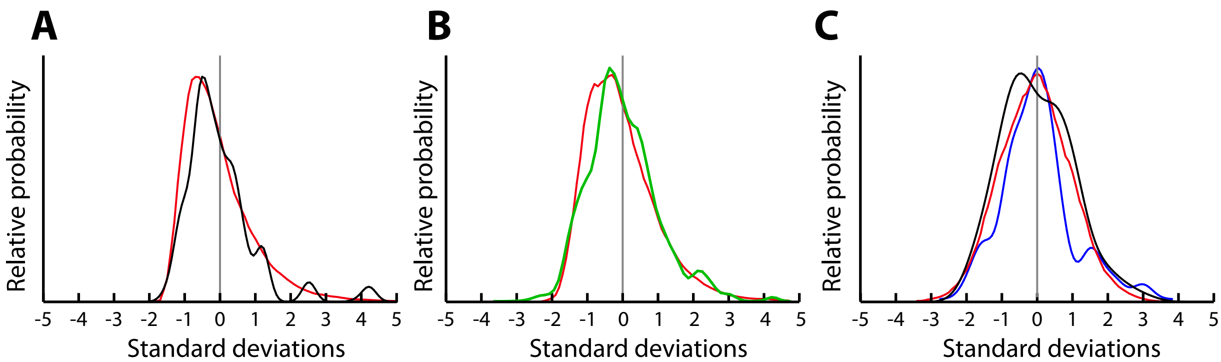

Figure DR2. Probability density distributions of selected normalized (unit variance and zero mean) sedimentation rate records and associated normalized synthetic records designed to model these geologic data. A, Kernel density estimation of decompacted sedimentation rates from ODP Site 980 as quantfied in Huybers (2007) (black curve). Red curve shows probability distribution of synthetic rates used in model 1 of main text designed to closely approximate the relatively strongly skewed Site 980 data. B, Green curve is the average kernel density estimation of an ensemble of Pleistocene decompacted sedimentation rate records, comprising data from: DSDP Site 607, Cores md900963, PC18, PC72, and ODP Sites 663, 664, 677, 846, 849, 925, 927, 980, 982, 983 (data from Huybers, 2007). Red curve shows probability distribution of synthetic rates used in model 2 of main paper, which closely matches the probability distribution of the ensemble. C, Kernel density estimation of sedimentation rates in Jurassic Kimmeridge Clay Formation (data from Huang et al., 2010, black curve) and Belemnite Marls (data in Weedon and Jenkyns, 1999, blue curve). Red curve shows probability distribution of synthetic rates used in model 3 of main paper. Both the synthetic record and the Kimmeridge Clay and Belemnite Marl data pass a Kolmogorov-Smirnov test for normality (p<0.05).

Site/Formation	Mean time span at which sedimentation rates determined (k.y.)	Length of record (k.y.)	Average sedimentation rate (cm/k.y.)	Coefficient of variation (* denotes an average (with range) from separate ~1 m.y. intervals)	Geologic age	Notes	Age model reference
DSDP607	24	2580	5.42	0.39	Pleistocene	Decompacted, depth derived age model	Huybers (2007)
md900963	24	1069.65	5.05	0.31	Pleistocene	Decompacted, depth derived age model	Huybers (2007)
ODP663	24	777.12	4.07	0.27	Pleistocene	Decompacted, depth derived age model	Huybers (2007)
ODP664	24	1067.43	4.18	0.35	Pleistocene	Decompacted, depth derived age model	Huybers (2007)
ODP677	24	1944	4.94	0.34	Pleistocene	Decompacted, depth derived age model, based on benthic δ18O record	Huybers (2007)
ODP846	24	1766.91	3.03	0.33	Pleistocene	Decompacted, depth derived age model	Huybers (2007)
ODP849	24	2576.42	2.96	0.27	Pleistocene	Decompacted, depth derived age model	Huybers (2007)
ODP925	24	1067.02	4.11	0.33	Pleistocene	Decompacted, depth derived age model	Huybers (2007)
ODP927	24	779.66	5.74	0.22	Pleistocene	Decompacted, depth derived age model, based on benthic δ18O record	Huybers (2007)
ODP980	24	1948.96	11.66	0.52	Pleistocene	Decompacted, depth derived age model	Huybers (2007)
ODP982	24	780	4.09	0.42	Pleistocene	Decompacted, depth derived age model, based on benthic δ18O record	Huybers (2007)
ODP983	24	1069.55	15.15	0.39	Pleistocene	Decompacted, depth derived age model	Huybers (2007)
PC18	24	778.04	1.75	0.38	Pleistocene	Decompacted, depth derived age model	Huybers (2007)
PC72	24	777.26	1.74	0.25	Pleistocene	Decompacted, depth derived age model	Huybers (2007)
Belemnite Marls	20	880	1.82	0.22	Pliensbachian	Uppermost 7.8 m of section not included to avoid systematic trend to lower rates	Weedon and Jenkyns (1999)
Kimmeridge Clay	36	6516	8.24	* 0.32 (0.23-0.38)	Kimmeridgian-Tithonian	Intermittantly laminated and sub-oxic	Huang et al. (2010)
ODP983	20	400	~14	~0.3	Pleistocene	Values quoted in Guyodo and Channell (2002), c.f. Huybers (2007) value for this site determined over longer interval	Guyodo and Channell (2002)
ODP659	20	5201.7	2.9	* 0.33 (0.32-0.35)	Plio-Pleistocene	Uppermost part of section not included to avoid potential influence of compaction	Tiedemann et al. (1994)
IODP1258	40	3381	0.92	* 0.25 (0.23-0.26)	Eocene	Stepwise changes in rates between 49.714 and 50.932 Ma not used to quantify coeffecient of variation	Sexton et al. (2011)

Table DR1. Table of sedimentation rate statistics for a range of stratigraphic successions. Coefficients of variation for each succession are calculated as the standard deviation of sedimentation rates divided by the mean rate (see main paper for details). For coefficients measured at astronomical time spans (20-40 k.y. in the above examples), values for both epicontinental (pre-Eocene) and oceanic successions range between 0.22 and 0.52 over *c*. million year intervals. Depth derived estimates of sedimentation rates (i.e. the Huybers, 2007 data) are not based on tuning of data to astronomical cycles, but rather are determined from a depth-tuned age model of δ^{18}O and geomagnetic events, which nonetheless have an estimated mean spacing of 24 k.y. (i.e. close to astronomical precession; see Huybers and Wunsch, 2004 and Huybers, 2007 for full details). Coefficients of variation for these depth-derived records likely constitute conservative estimates of sedimentation rate unsteadiness because the unsteadiness is quantified relative to the mean spacing between δ^{18}O and geomagnetic events of all the records studied (see p.39 of Huybers, 2007). Although not designed to be an exhaustive list, these examples have broadly consistent sedimentation rate variability (mean coefficient of variation ~0.33, standard deviation ~0.074). As far as possible, stepwise changes in rates and systematic trends have been avoided in order to provide a handle on unsteadiness pertaining to natural variability without obvious extrinsic control. In Pleistocene records, rate variability at astronomical scales may be linked to glacial-interglacial scale variability, as discussed in Guyodo and Channell (2002) in the case of ODP Site 983. Note also that the successions analyzed are typically bioturbated. Bioturbation and the consequent smoothing of rate variability may lead to an underestimation of the true unsteadiness of sedimentation operative at the time of deposition before mixing.

References cited

Crowley, K.D., Duchon, C.E., and Rhi, J., 1986, Climate record in varved sediments of the Eocene Green River Formation: Journal of Geophysical Research, v. 91, p. 8637-8647.
Guyodo, Y., and Channell, J.E.T., 2002, Effects of variable sedimentation rates and age errors on the resolution of sedimentary paleointensity records: Geochemistry, Geophysics, Geosystems, v. 3, doi: 10.1029/2001GC000211.
Huang, C., Hesselbo, S.P., and Hinnov, L., 2010, Astrochronology of the late Jurassic Kimmeridge Clay (Dorset, England) and implications for Earth system processes: Earth and Planetary Science Letters, v. 289, p. 242-255.
Huybers, P., 2007, Glacial variability over the last two million years: an extended depth-derived agemodel, continuous obliquity pacing, and the Pleistocene progression: Quaternary Science Reviews, v. 26, p. 37-55.
Huybers, P., and Wunsch, C., 2004, A depth-derived Pleistocene age model: Uncertainty estimates, sedimentation variability, and nonlinear climate change: Paleoceanography, v. 19, doi:10.1029/2002PA000857.
Sexton, P.F., Norris, R.D., Wilson, P.A., Palike, H., Westerhold, T., Röhl, U., Bolton, C.T., and Gibbs, S., 2011, Eocene global warming events driven by ventilation of oceanic dissolved organic carbon: Nature, v. 471, p. 349-352.
Tiedemann, R., Sarnthein, M., and Shackleton, N.J., 1994, Astronomic timescale for the Plioecene Atlantic $\delta^{18}O$ and dust flux records of Ocean Drilling Program Site 659: Paleoceanography, v. 9, p. 619-638.
Weedon, G.P., and Jenkyns, H.C., 1999, Cyclostratigraphy and the Early Jurassic timescale: Data from the Belemnite Marls, Dorset, southern England: Geological Society of America Bulletin, v. 111, p. 1823-1840.